Soumyajit Goswami[1] / Arghya Sarkar[2] / Samarjit Sengupta[3]

Digital Metering of Electrical Power Components Using Adaptive Non-Uniform Discrete Short Time Fourier Transform

[1] IBM India Private Limited, Saltlake, Sector V, Kolkata 700091, West Bengal, India, E-mail: soumyajit_goswami@yahoo.com. https://orcid.org/0000-0001-8911-9603.
[2] Electrical Engineering, MCKV institute of Engineering, Howrah, West Bengal, India
[3] Applied Physics, University of Calcutta, Kolkata, West Bengal, India

Abstract:
This paper presents an adaptive Goertzel filter bank based discrete short time Fourier transform (DSTFT) implementation algorithm, called adaptive non-uniform discrete short time Fourier transform (ANDSTFT) for online measurement of electrical power components using IEEE Standard 1459–2010. The proposed ANDSTFT algorithm utilizes effective combination of non-uniform discrete Fourier transform (NDFT) and window method to detect the spectrum of each individual finite short time segment of power signals at distinct, arbitrarily located frequencies. Compared with the well-established technique such as windowed FFT interpreted DSTFT based approaches, the proposed method offers (i) better accuracy (ii) higher degree of immunity and insensitivity to noise, and (iii) reduced computational complexity per sample interval. The simulation results have been given and its response time and accuracy have been compared with the conventional windowed FFT interpreted DSTFT based techniques. Real-time implementation of the proposed approach has also been presented.

Keywords: Goertzel algorithm, harmonics, discrete short time Fourier transform, power measurements, IEEE Standard 1459–2010

DOI: 10.1515/ijeeps-2018-0283

Received: October 17, 2018; **Revised:** June 6, 2019; **Accepted:** July 1, 2019

1 Introduction

The estimation of power components like active, reactive and apparent power under non-sinusoidal condition play very important role in power system equipment development, tariff assessment and compensation technique design. The IEEE Standard 1459–2010 [1] provides most comprehensive guidelines for power component measurement using distorted power system signals. Based on this standards, different techniques and algorithms have been proposed in literature, for example the discrete Fourier transform (DFT) based algorithm [2–4], the discrete wavelet transforms (DWT) based approach [5], Newton type algorithm [6], time domain techniques [7], adaptive linear neuron (ADALINE) based methods [8] etc. The search for highly accurate and computationally efficient techniques still continues.

The non-uniform discrete short time Fourier transform (NSTFT) based harmonic analysis are proposed in [9, 10]. These algorithms provide excellent accuracy to estimate the spectrum at nominal system frequency. However, the main shortcoming of these approaches is that, it avoids the key issue spectral leakage and consequently fails to analyze real time power system signals during off-nominal frequency conditions. To overcome the above-mentioned limitation and utilize the promising approach for real time power components estimation (nominal or off-nominal conditions), the following modifications are proposed in this paper:

1. Window length of short time Fourier transform is adaptively changed in accordance with system fundamental frequency to reduces the possibility of spectral leakage.
2. At off-nominal frequency conditions, the adaptive window length may be nearly equal but not exactly equal to the integer multiple of input signal period. Hence, proper window function has been utilized for further reduction of the spectral leakage effect.
3. Reformulation of power component definition contained in the IEEE Standard 1459–2010 [1] at the presence of window function.

Soumyajit Goswami is the corresponding author.

Since the Fourier coefficients of adaptively selected short time section have been computed on selected frequencies, the modified approach is termed as "adaptive non-uniform discrete short time Fourier transform" (ANDSTFT).

The advantages of the proposed ANDSTFT in comparison with the conventional FFT based DSTFT [4] are:

1. The ANDSTFT enables to compute the Fourier coefficients of the input signal at any arbitrary points in frequency domain (not only at equally spaced integer points like the FFT) without changing the algorithm structure. This is predominantly useful for sub-harmonic and inter-harmonic estimations and spectrum analysis at off-nominal frequency conditions.
2. The proposed algorithm is proficient to estimate spectrum at the selected frequencies, calculation of entire points in frequency domain need not be necessary. Hence, slight idea about the harmonic orders of the distorted signals significantly reduces the computational complexity. However, Table 1 shows that the computational load per sample interval of the proposed algorithm is also less than that of the FFT based DSTFT, when all the frequency points have been considered.
3. The ANDSTFT has capacity of doing sample by sample processing, thus, suitable for real time implementation. Moreover, computational complexity per sample is less.
4. The adaptive selection of window length (not only power of two) substantially reduces spectral leakage effect.

Theoretical aspects and advantages of the proposed ANDSTFT have been discussed, the power components measurement accuracy is evaluated, and the simulation results are presented. LabVIEW™ based test results also provided to establish the feasibility of the proposed method in real time. The acquired results confirm an advantage in improved accuracy, better immunity and insensitivity to noise, and lower computational load per sample interval, than the conventional FFT interpreted DSTFT based approaches.

2 Theoretical development

This paper proposes a modified algorithm, called adaptive non-uniform discrete short time Fourier transform (ANDSTFT) for online implementation of the discrete short time Fourier transform (DSTFT). In this section, the theoretical development of ANDSTFT is briefly explained.

2.1 Definition of the adaptive non-uniform discrete short time fourier transform (ANDSTFT)

The ANDSTFT evaluates the frequency samples of finite length "snap-shot" sequence at H arbitrary, distinct points in z-plane. If the adaptive window be of length N_{Adp}, defined in the range $0 \leq m \leq N_{Adp}$, the ANDSTFT of the discrete time signal $x[n]$ has been defined at a particular time index, n, as

$$X_{ANDSTFT}\left[z_h, n\right] = \sum_{m=0}^{N_{Adp}} x\left[m\right] w\left[n-m\right] z_h^{-m}\,,\ 0 \leq m \leq N_{Adp} \tag{1}$$

where $z_1, \ldots, z_H$ are distinct points located arbitrarily in the z-plane within unit circle.

2.2 Real time implementation of the ANDSTFT

The proposed ANDSTFT implementation algorithm consists of the following steps:

2.2.1 Determining the fundamental frequency and integer multiple of the input signal periods with minimum possible error

For the purpose of precise estimation of the fundamental frequency of power system signals with lower computational load, a second-degree digital integrator based method [11] is effectively used. Pre-filtration of non-sinusoidal signal $s\left[n\right]$ by a suitable band-pass filter eliminates dc offset and higher order harmonics; and leads following observation model

$$s_F[n] = \sqrt{2}S_1 \sin(\omega_1 n + \alpha_F) + \xi_F[n] \tag{2}$$

where $\sqrt{2}S_1$ is the amplitude, n is the number of samples, ω_1 is the fundamental angular frequency, α_F is the phase and $\xi_F[n]$ is the noise signal.

In [11], the authors present a novel approach for fast and accurate estimation of fundamental frequency from eq. (2) with modest computation. This algorithm is highly robust with respect to distortion and noise, and efficiently takes care of proximity to zero crossing problems.

The fundamental frequency f within the observation window can be obtained utilizing [11] as:

$$f[n] = \frac{1}{2\pi}\sqrt{r[n]} \tag{3}$$

where,

$$\hat{r}[n] = \frac{\sum_{j=0}^{A-1} s_F[n-j]\{-s_{FIBPF}[n-j]\}}{\sum_{j=0}^{A-1} (s_{FIBPF}[n-j])^2} \tag{4}$$

$s_{FIBPF}[n]$ is the band-pass second-degree integration of $s_F[n]$, A is the length of the observation window.

If, N_{Adp} is the nearest integer number of samples within p periods of the input signal corresponding to the estimated integer multiple of input signal periods, then from the knowledge of the system fundamental frequency, f, it can be defined as

$$N_{Adp} = \text{round}(pf_s/f) \text{ to the nearest integer.} \tag{5}$$

to the nearest integer.

Hence, N_{int} is adaptively changed in dependence on the value of system fundamental frequency and reduces the possibility of spectral leakage.

2.2.2 Application of window function to the input signal

The advantage of application of window functions is to diminish the spectral leakage at a great extent, which in turn allows to analyze the periodical signal without necessity to determine integer multiple of its periods. The two frequency domain parameters characterizing the Fourier transform of a window function are its main lobe width and the relative side lobe amplitude. The former parameter concludes the ability of the window to resolve two signal components in the vicinity of each other, while the latter controls the degree of leakage of one component into a nearby signal component. Among different types of window functions, Hanning and Hamming windows seem particularly suitable for harmonic and inter harmonic estimation at the presence of spectral leakage because both are characterized by a main lobe width exactly double and side lobe width exactly equal compared to those of rectangular window [12]. Application of window function $w(n)$ to N_{Adp} samples of the input signal $x(n)$ gives:

$$x_e[n] = x[n]\,w[n] \;\; n = 0, 1, 2, ..., N_{Adp} \tag{6}$$

However, the application of Hanning or Hamming window requires an additional narrowband correction factor to boost the peak level to match the rectangular window peak level [12].

2.2.3 Computation of the ANDSTFT coefficients of weighted input signal

A combined approach has been proposed for real time estimation of the ANDSTFT coefficients, in which it has been assumed that the window is fixed and, within each and every short time segment of the signal, the frequencies of interest are also fixed and located on the unit circle in the z-plane. Under these conditions, for

a specific short time section, $X_{ANDSTFT}[z_h,n]$ is simply the normal NDFT of the sequence $x_e[n]$ and can be implemented using the Goertzel algorithm due to its lower computational complexity and sample by sample computation [13]. Goertzel's algorithm allows to compute every single bit of the ANDSTFT with the second order recursive digital filters. The output $y_h[n]$ of this algorithm is the output of initially relaxed LTI digital filter with a transfer function [9, 10],

$$H_h(z) = \frac{1}{1 - W_H^h z^{-1}} \tag{7}$$

with an input signal $x_e[n]$. The block diagram of modified approach to the recursive computation of h^{th} DFT sample of eq. (7) is shown in Figure 1.

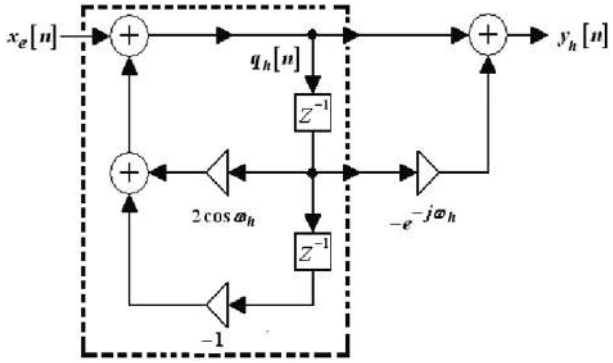

Figure 1: Goertzel algorithm as a second order recursive computation.

In the proposed approach, the intermediate signals, $q_h[n]$ and $q_h[n-1]$ of Figure 1 are computed recursively using the difference equation

$$q_h[n] = x_e[n] + 2\cos\left(\frac{2\pi hp}{N_{int}}\right)\omega_h \times q_h[n-1] - q_h[n-2], 0 \le n \le N \tag{8}$$

with the initial conditions

$$q_h[-1] = q_h[-2] = 0 \tag{9}$$

and ω_h is adaptively chosen as

$$\omega_h = hf/f_s \tag{10}$$

The ANDSTFT coefficients have been computed at $N_{Adp}{}^{\text{th}}$ iteration using the following expression

$$X_{ANDSTFT}[z_h,n] = y_h[n]|_{n=N_{Adp}} = q_h\left[N_{Adp}\right] - e^{-j\left(2\pi hp/N_{Adp}\right)}q_h\left[N_{Adp}-1\right] \tag{11}$$

If, the signal energy is distributed in H distinct but arbitrarily placed points over the unit circle in z-plane, then the spectral analysis of the signals using the ANDSTFT can be performed using a bank of H adaptive Goertzel IIR filters (one per harmonic of interest).

The block diagram of the proposed ANDSTFT algorithm has been shown in Figure 2 whereas the flow chart of the proposed algorithm has been presented in Appendix.

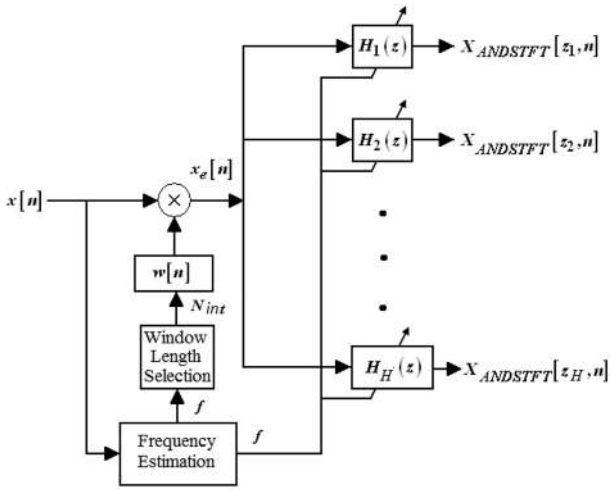

Figure 2: Realization of the ANDSTFT using the adaptive Goertzel filter bank.

2.3 Computational complexity

For real input signals, N point FFT based DSTFT algorithm waits entire window cycle to accrue weighted data points and performing the FFT operation using $(N/2)\log 2N$ complex multiplications and $N\log 2N$ complex additions [10] within a sample interval, after completion of each window. For windowing operation, it also requires N real multiplications.

Whereas, H point ANDSTFT ($H \leq N$) requires $H+1$ real multiplications and $2H$ real additions (excluding computational load of frequency measurement) at every sample interval except end sample period of each window cycle. At end sample, it computes recursive as well as non-recursive portion of Figure 1; hence requires $H+1$ real multiplications, $2H$ real additions, H multiplications between real and complex numbers, and H complex additions.

Considering one complex multiplication encompasses four real multiplications and two real additions, and one complex addition encompasses two real additions, the complexities of both algorithms for $N=256$ are summarized in Table 1. For fair comparison, the worst case has been considered where all 256 bins have been calculated using the ANDSTFT ($H=N$).

Table 1: Computational complexities of ANDSTFT and FFT based DSTFT for real input signal.

$N = 256$	At every sample interval between first to last but one sample interval of window sequence		Last Sample interval of window sequence		Total Computational Load per window cycle	
	Real Additions	Real Multiplications	Real Additions	Real Multiplications	Real Additions	Real Multiplications
ANDSTFT (excluding computational load of fundamental frequency measurement)	512	257	1024	769	132,096	66,561
FFT based STFT	–	1	6144	4097	6144	4352

From Table 1 it has been observed that the total computational load per window cycle of the ANDSTFT is much larger than the FFT based DSTFT. When computation per sample interval has been considered, the application of the ANDSTFT is much more beneficial. In an on-line estimation process, the mathematical calculation corresponding to a particular sample has to be performed within the sample time interval between this particular sample and the next sample. Since windows are not overlapped in the developed algorithm (as shown in Appendix), processor choice depends on maximum mathematical operation requirement within a single sample interval, not on total computational load. Hence, for fixed sampling frequency and fixed N, the proposed ANDSTFT algorithm can easily be implemented in a relatively slower processor, thus in turn reduces the instrument cost.

Moreover, the computational load of the fundamental frequency estimation algorithm does not pose too many problems. As shown in flow chart of the proposed algorithm, at every sample interval except end sample period of each window cycle requires 8 real additions and 9 real multiplications for band pass filtration, 8 real additions and 9 real multiplications for band-pass second-degree integration, 2 real additions and 2 real multiplications to compute C and D. Hence, only extra 18 real additions and 20 real multiplications per sample interval are required for fundamental frequency estimation. Computational complexities at last sample interval of window sequence is slightly greater, since along with C and D, r and f to be calculated.

In practice, power system signals contain only a few dominant harmonics [1]. In this case the ANDSTFT approach is more efficient from total computational load view point, since for a small number of filters, the computational complexity will be much lower than the conventional FFT based STFT, even with the log(N) advantage.

2.4 The ANDSTFT stability

Every ANDSTFT single bin Goertzel filter is marginally stable since its poles lie on the unit circle in z-plane. If filter coefficient numerical rounding errors are not severe, the ANDSTFT is bounded-input-bounded-output (BIBO) stable [13]. However, if rounding causes the filter's poles to move outside the unit circle, a damping factor d can be utilized to force the poles to be at a radius of d inside the unit circle [13]. Use of the damping factor d confirms stability, but the output of the Goertzel filter is no longer exactly equal to $X_{ANDSTFT}[z_h, n]$. While the error is reduced by making d very close to (but less than) unity, a scheme does exist for eliminating that error at the expense of additional logic operations.

3 Reformulation of the power components' definitions using the ANDSTFT

This section provides single-phase power components' definitions contained in the IEEE Standard 1459–2010 [1] and their reformulation in the ANDSTFT domain under non-sinusoidal situations. The basic assumption is that the periodic power system signals have been uniformly sampled at sampling frequency fs, greater than the Nyquist rate, so that aliasing of spectra does not occur. The expressions of power components definitions in the ANDSTFT domain are only provided here; details derivation may be found in [10].

At steady state conditions, the non-sinusoidal instantaneous voltage, v, and current, i, of fundamental angular frequency ω1 may be represented by Fourier series of the form:

$$v = \sqrt{2}V_1 \sin(\omega_1 t - \alpha_1) + \sqrt{2}\sum_{h\neq 1} V_h \sin(\omega_h t - \alpha_h) = v_1 + v_H \tag{12}$$

$$i = \sqrt{2}I_1 \sin(\omega_1 t - \beta_1) + \sqrt{2}\sum_{h\neq 1} I_h \sin(\omega_h t - \beta_h) = i_1 + i_H \tag{13}$$

where v_1, i_1 represent the power system frequency components, and v_H, i_H represent the harmonic components. α_1,β_1 correspond to the fundamental voltage and current phase angle respectively, while α_h and β_h represent the harmonic voltage and current phase angle respectively, at h^{th} harmonic.

3.1 RMS calculations

The RMS values of the non-sinusoidal voltage signals with time period T is

$$V_{rms} = \frac{1}{kT}\int_{\tau}^{\tau+kT} v^2 dt = \sqrt{V_1^2 + V_H^2} \tag{14}$$

where

$$\begin{aligned} V_1 &= \tfrac{1}{kT}\int_{\tau}^{\tau+kT} v_1^2 dt \\ &= \tfrac{\sqrt{2}}{\eta N}\sqrt{\left(\mathrm{Re}\left\{V_{ANDSTFT}\left[z_1,n\right]\right\}^2 + \mathrm{Im}\left\{V_{ANDSTFT}\left[z_1,n\right]\right\}^2\right)} \end{aligned} \tag{15}$$

$$\begin{aligned} V_H &= \tfrac{1}{kT}\int_{\tau}^{\tau+kT} v_H^2 dt \\ &= \tfrac{\sqrt{2}}{\eta N}\sqrt{\sum_{\substack{h=0\\h\neq 1}}^{M_v} \mathrm{Re}\left\{V_{ANDSTFT}\left[z_h,n\right]\right\}^2 + \mathrm{Im}\left\{V_{ANDSTFT}\left[z_h,n\right]\right\}^2} \end{aligned} \tag{16}$$

M_v is the maximum order of the voltage harmonics, η is the narrowband correction factor, needed to match any given window peak level to the rectangular window peak level. It is defined as the ratio of the window integral to the integral of a rectangular window of same length.

$$\eta = \frac{\sum_{i=0}^{N} w_i}{\sum_{i=0}^{N} w_{rect_i}} = \frac{1}{N}\sum_{i=0}^{N} w_i \tag{17}$$

Similarly, the expressions of rms value of distorted current signal is

$$I_{rms} = \frac{1}{kT}\int_{\tau}^{\tau+kT} i^2 dt = \sqrt{I_1^2 + I_H^2} \tag{18}$$

where

$$\begin{aligned} I_1 &= \tfrac{1}{kT}\int_{\tau}^{\tau+kT} i_1^2 dt \\ &= \tfrac{\sqrt{2}}{\eta N}\sqrt{\mathrm{Re}\left\{I_{ANDSTFT}\left[z_1,n\right]\right\}^2 + \mathrm{Im}\left\{I_{ANDSTFT}\left[z_1,n\right]\right\}^2} \end{aligned} \tag{19}$$

$$\begin{aligned} I_H &= \tfrac{1}{kT}\int_{\tau}^{\tau+kT} i_H^2 dt \\ &= \tfrac{\sqrt{2}}{\eta N}\sqrt{\sum_{\substack{h=0\\h\neq 1}}^{M_i} \mathrm{Re}\left\{I_{ANDSTFT}\left[z_h,n\right]\right\}^2 + \mathrm{Im}\left\{I_{ANDSTFT}\left[z_h,n\right]\right\}^2} \end{aligned} \tag{20}$$

M_i is the maximum order of current harmonics.

3.2 Active power

The total active power P, fundamental active power P_1 and harmonic active power P_H can be derived as

$$P = \frac{1}{kT}\int_{\tau}^{\tau+kT} v_{rms} i_{rms} dt \tag{21}$$

$$\begin{aligned} P_1 &= \tfrac{1}{kT}\int_{\tau}^{\tau+kT} v_1 i_1 dt \\ &= \tfrac{2}{N^2\eta^2}\left(\mathrm{Re}\left\{V_{ANDSTFT}\left[z_1,n\right]\right\}\mathrm{Re}\left\{I_{ANDSTFT}\left[z_1,n\right]\right\}\right. \\ &\quad \left. + \mathrm{Im}\left\{V_{ANDSTFT}\left[z_1,n\right]\right\}\mathrm{Im}\left\{I_{ANDSTFT}\left[z_1,n\right]\right\}\right) \end{aligned} \tag{22}$$

$$\begin{aligned} P_H &= \tfrac{1}{kT}\int_{\tau}^{\tau+kT} v_H i_H dt \\ &= \tfrac{2}{N^2\eta^2}\sum_{h\neq 1}\left(\mathrm{Re}\left\{V_{ANDSTFT}\left[z_h,n\right]\right\}\mathrm{Re}\left\{I_{ANDSTFT}\left[z_h,n\right]\right\}\right. \\ &\quad \left. + \mathrm{Im}\left\{V_{ANDSTFT}\left[z_h,n\right]\right\}\mathrm{Im}\left\{I_{ANDSTFT}\left[z_h,n\right]\right\}\right) \end{aligned} \tag{23}$$

3.3 Reactive power

The fundamental reactive power Q_1 is

$$\begin{aligned} Q_1 &= \frac{\omega_1}{kT_2}\int_{\tau}^{\tau+kT} i_1\left[\int v_1 dt\right]dt \\ &= \frac{2}{N^2\eta^2}\left(\mathrm{Re}\left\{I_{ANDSTFT}\left[z_1,n\right]\right\}\mathrm{Im}\left\{V_{ANDSTFT}\left[z_1,n\right]\right\}\right. \\ &\quad \left.-\mathrm{Re}\left\{V_{ANDSTFT}\left[z_1,n\right]\right\}\mathrm{Im}\left\{I_{ANDSTFT}\left[z_1,n\right]\right\}\right) \end{aligned} \tag{24}$$

Budeanu's reactive power can be expressed as

$$\begin{aligned} Q_B &= \frac{2}{N^2\eta^2}\sum_{h}\left(\mathrm{Re}\left\{I_{ANDSTFT}\left[z_h,n\right]\right\}\mathrm{Im}\left\{V_{ANDSTFT}\left[z_h,n\right]\right\}\right. \\ &\quad \left.-\mathrm{Re}\left\{V_{ANDSTFT}\left[z_h,n\right]\right\}\mathrm{Im}\left\{I_{ANDSTFT}\left[z_h,n\right]\right\}\right) \end{aligned} \tag{25}$$

3.4 Apparent power

Once voltage and current definitions at the ANDSTFT domain are known, definitions of the fundamental apparent power (S_1), total apparent power(S), nonfundamental apparent power (S_N) and nonactive power(N) can easily be reformulated by substituting the corresponding values from eqs. (13), (17), (12) and (16) in the following definitions:

$$S_1 = V_1 I_1 \tag{26}$$

$$S = V_{rms} I_{rms} \tag{27}$$

$$S_N = \sqrt{S^2 - S_1^2} \tag{28}$$

$$N = \sqrt{S^2 - P^2} \tag{29}$$

4 Algorithm testing

A set of simulation tests has been performed in MATLAB environment to estimate the validity and performance of the proposed algorithm under different operating conditions. The power components for each of the cases have been computed by the proposed two cycles ANDSTFT based algorithms and compared with the results obtained from the conventional 256-point FFT interpreted DSTFT based approaches. To reduce leakage effect, both algorithms utilize Hanning window function.

4.1 Static test

In order to determine the sensitivity of the proposed algorithm on the sampling frequency, the following input voltage and current signals are processed:

$$\begin{aligned} v(t) &= \sqrt{2}\left[1.0\sin\left(2\pi f t\right) + 0.03\sin\left(6\pi f t + 135^\circ\right)\right. \\ &\quad \left. + 0.01\sin\left(10\pi f t + 150^\circ\right) + 0.01\sin\left(14\pi f t + 140^\circ\right)\right] \end{aligned} \tag{30}$$

$$\begin{aligned} i(t) &= \sqrt{2}\left[1.0\sin\left(2\pi f t + 10^\circ\right) + 0.3\sin\left(6\pi f + 150^\circ\right)\right. \\ &\quad \left. + 0.2\sin\left(10\pi f t + 135^\circ\right) + 0.1\sin\left(14\pi f t - 22.5^\circ\right)\right] \end{aligned} \tag{31}$$

The fundamental frequency f is kept constant at 50 Hz and the sampling frequency has been varied in the range, 800 to 25,600 Hz power components at each of the cases are estimated. The modulus of percent errors in P, Q_B and S measurements, termed as eP, eQ and eS, respectively, have been shown in Figure 3.

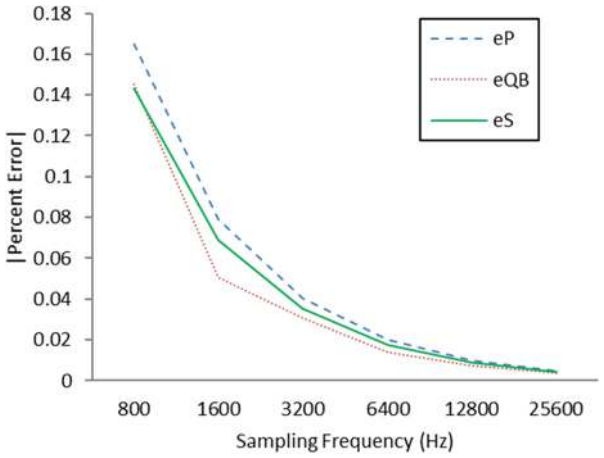

Figure 3: Absolute percent errors in power components estimation with the sampling frequency.

From the figure it can be concluded that the absolute percent errors in power components estimation is gradually decreases with increase in sampling frequency. Cconsidering 50 Hz nominal frequency, the sampling frequency has been chosen at 6.4 kHz to get the effect of harmonics up to 64th order as well as moderate accuracy.

In order to test algorithms static accuracy under off-nominal frequency condition, the fundamental frequency f of input signals [eqs. (30) and (31)] has been varied in the range, 48 to 51 Hz in steps of 0.2 Hz. The eP, eQ and eS, have been depicted in Figure 4, which exhibits that the proposed ANDSTFT based algorithm provides much better accuracy than the DSTFT based approaches during frequency off-set condition.

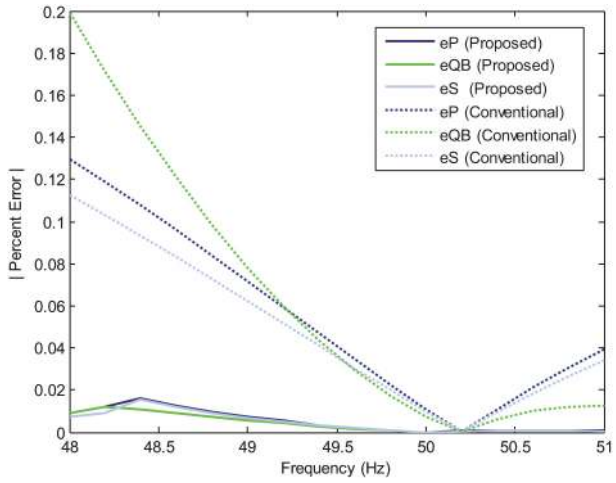

Figure 4: Absolute percent errors in power components estimation under off-nominal frequency condition.

4.2 Noise test

The same input signals [eqs. (30) and (31)]; with the superimposed zero-mean white noise has been utilized as input test signals. A range from a highly noisy signal (SNR = 20 dB) to a low noisy signal (SNR = 60 dB) is covered and, in each case, the steady-state error is measured using the proposed algorithm; and compared to the DSTFT based techniques. The absolute peak of oscillating steady state errors in active power measurement have been depicted in Figure 5, which exhibits that the error rapidly drops from SNR = 20 dB to SNR = 60 dB and the proposed algorithm provides better immunity to noise than the DSTFT based approach. The sensitivity of noise of both the algorithms can be decreased by increasing the data window size but at the cost of prolonged dynamic response time.

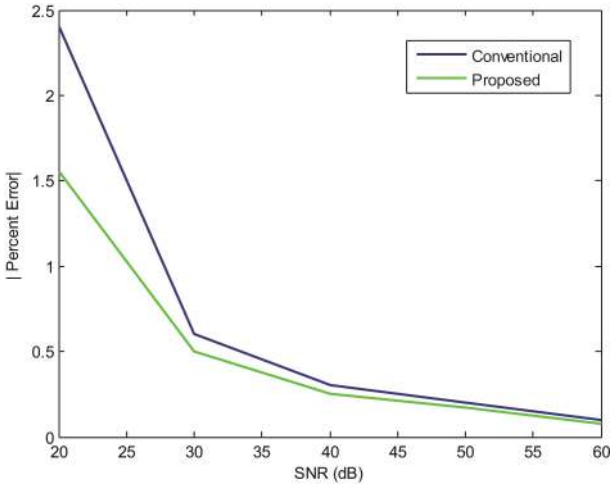

Figure 5: Absolute maximum steady-state errors in active power estimation in terms of the SNR.

4.3 Dynamic test

An experimental dynamic condition has been achieved by considering the following input voltage and current signals:

$$\begin{aligned} v(t) &= \cos\left(2\pi ft + 45^\circ\right) + 0.5\cos\left(10\pi ft + 120^\circ\right) \\ &\quad + 0.3\cos\left(14\pi ft + 150^\circ\right) + 0.2\cos\left(22\pi ft + 280^\circ\right) \end{aligned} \tag{32}$$

$$\begin{aligned} i(t) &= \cos\left(2\pi ft\right) + 0.4\cos\left(10\pi ft + 60^\circ\right) \\ &\quad + 0.2\cos\left(14\pi ft + 30^\circ\right) + 0.1\cos\left(22\pi ft + 130^\circ\right) \end{aligned} \tag{33}$$

In the period from $t = 0$ to 0.25s, both the test signals were pure cosine signals and consisted of the first terms from eqs. (30) and (31). At $t = 0.25$s, both input signals are distorted with higher harmonics as given by eqs. (32) and (33). Simultaneously, the frequency of the fundamental harmonic is instantaneously changed from 50 to 40 Hz. The tracking of power components using the proposed ANDSTFT based algorithm have been depicted in Figure 6. In the period before the distortion is applied, $S = 0.5$ p.u., and $P = Q = 0.5/\sqrt{2} = 0.3535$ p.u. After a convergence period of about four cycles, true estimates of the new power components are obtained (P = 0.3799 p.u., $Q_B = 0.4711$ p.u., and $S = 0.6461$ p.u.). The transient features of the fundamental frequency estimation algorithm mainly influence the response time of the proposed algorithm. The conventional DSTFT based approaches also take same transient time as that of the proposed one. Since, sampling frequency (6.4 kHz) is the integer multiple of both fundamental frequencies (50 Hz and 40 Hz), both algorithms provide high accuracy at steady state, before and after step change has occurred.

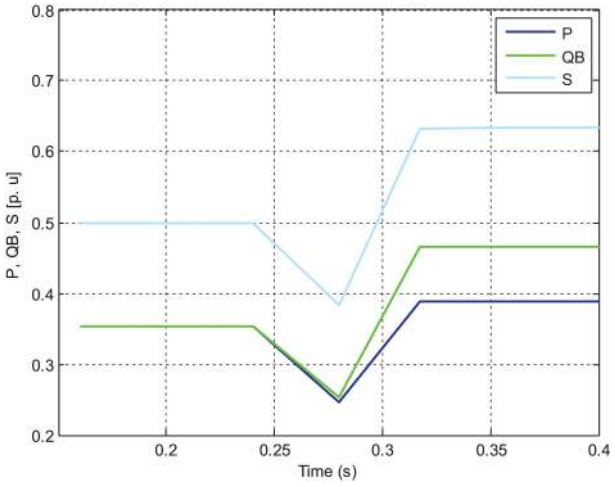

Figure 6: Estimated power components (dynamic test) by the ANDSTFT based algorithms.

5 Real-time implementation using LabVIEW

5.1 Experimental setup

The proposed algorithm has been implemented using virtual instrument developed in LabVIEW and tested in the laboratory to establish its feasibility in a real-time environment. The laboratory setup is shown in Figure 7.

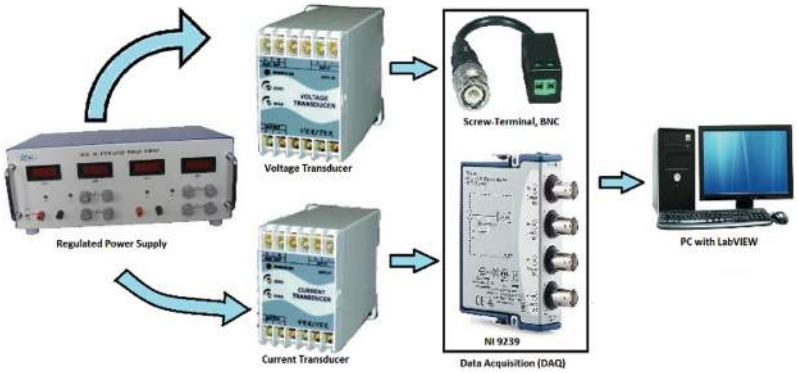

Figure 7: Laboratory test setup using LabVIEW for power components measurement.

The components used are as follows:

1. Regulated Power Supply: ±12 V and ±15 V for voltage and current transducers respectively
2. LEM Voltage Transducer: rms voltage 600 V, rms current 10 mA, conversion ration 600 V: 25 mA, ±0.8 % accuracy
3. LEM Current Transducer: rms current 0.25A, conversion ratio 100: 1000, ±0.5 % accuracy
4. NI 9239 Data Acquisition (DAQ) Card: 4-Channel, 24-Bit, ±10 V signal levels, 50 kS/s/ch sample rate
5. Bus: ARM Electronics VC4 Mini Screw Terminal Balunwith 4 BNC Cord
6. Computer: Dual Core Intel® Pentium 4, 3.4 GHz CPU, 512 K Cache, 64-Bit
7. LabVIEW™ Software for Windows: LabVIEW 2015 Service Pack 1

The system software has been entirely implemented using the LabVIEW graphical programming language. The data acquisition program performs continuous data acquisition of the voltage and current signals, whereas the harmonic measuring program and analyzing programs carry out computation of the harmonic parameters with power components [14].

5.2 Experimental results

Power signal harmonics are estimated and power components at off-nominal frequency ($f = 48$ Hz) are measured, as shown in Figure 8, using a set of functions provided by LabVIEW.

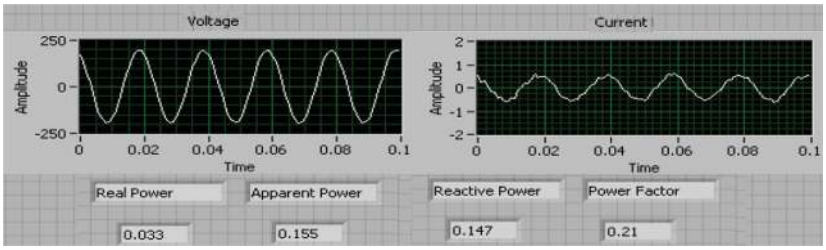

Figure 8: Power components measurement.

While comparing with ANDSTFT and DSTFT, it has been revealed that the proposed method provides much better accuracy (percent errors is of the order of 10^{-12} %) than the conventional DSTFT based approach (percent errors is of the order of 10^{-2} %), presented in Table 2.

Table 2: Power components estimation at nominal frequency.

		IEEE Standard Definitions	ANDSTFT based Definitions Measured Values	% error	DSTFT based Definitions Measured Values	% error
RMS	V_1	1.0000	1.0000	−5.8e-013	1.0000	−0.0045
	V_{rms}	1.0005	1.0005	−6e-013	1.0006	−0.0046
	I_1	1.0000	1.0000	-e-016	1.0001	−0.0051
	I_{rms}	1.0677	1.0677	−6e-15	1.0678	−0.0051
Active power	P_1	0.9848	0.9848	−5e-013	0.9849	−0.0100
	P	0.9945	0.9945	−5e-013	0.9946	−0.0111
Reactive power	Q_1	−0.1736	−0.1736	−2e-012	−0.1736	0.0043
	Q_B	−0.17516	−0.17516	−2.2e-012	−0.1752	0.0075
Apparent power	S_1	1.0000	1.0000	−6e-013	1.0001	−0.0096
	S	1.0683	1.0683	−5e-013	1.0684	−0.0097
	S_N	0.3758	0.3758	−6e-013	0.3759	−0.0102
	N	0.3902	0.3902	−1.1e-012	0.3902	−5e-04

6 Conclusion

A modified algorithm for the digital metering of power components according to IEEE Standard 1459–2010 is presented and tested in detail. It is based on the application of the ANDSTFT, which is a modified approach for real time implementation of the DSTFT. The ANDSTFT is able to synchronize itself with system frequency and can estimate the spectrum at the exact harmonic order of interest. The algorithm has been tested both simulation and hardware platform. The obtained results confirm an advantage in improved accuracy during off-nominal frequency conditions, better immunity to noise, and lower computational load per sample interval, than the popular FFT interpreted DSTFT based approaches. Like the DSTFT, the projected approach also takes almost four cycles to reach steady state after sudden change in the harmonic amplitude or system fundamental frequency. The developed scheme is highly reliable and possesses enough flexibility to suit the requirement of different real time systems.

Nomenclature

eP modulus of percent error in P

eQ modulus of percent error in Q_B

eS modulus of percent error in S

f fundamental frequency of power system signals

f_s sampling frequency

$i\,(t)$ instantaneous current of single-phase system

i_1 power system frequency component of single-phase current signal

I_{rms} rms current of single-phase system

I_1 fundamental rms current of single-phase system

i_H harmonic components of single-phase current signal

I_H harmonic rms current of single-phase system

I_h single-phase rms current at h^{th} harmonic

N window length

N_{int} nearest integer number of samples

n number of samples

P total active power

P_1 fundamental active power

P_H harmonic active power

P_N nonactive power
Q total reactive power
Q_1 fundamental reactive power
Q_B Budeanu's reactive power
S total apparent power
S_1 fundamental apparent power
S_N nonfundamental apparent power
t time
T time period
V_{rms} rms voltage of single-phase system
$v(t)$ instantaneous voltage of single-phase system
v_1 power system frequency component of single-phase voltage signal
V_1 fundamental rms voltage of single-phase system
v_H harmonic components of single-phase voltage signal
V_H harmonic rms voltage of single-phase system
V_h single-phase rms voltage at h^{th} harmonic
α_1 fundamental voltage phase angle single-phase system
α_h voltage phase angle of single-phase system at h^{th} harmonic
β_1 fundamental current phase angle of single-phase system
β_h current phase angle of single-phase system at h^{th} harmonic
ω_1 fundamental angular frequency
$\xi_F[n]$ zero mean random noise of $s[n]$

Appendix

Flow Chart of the ANDSTFT Implementation Algorithm

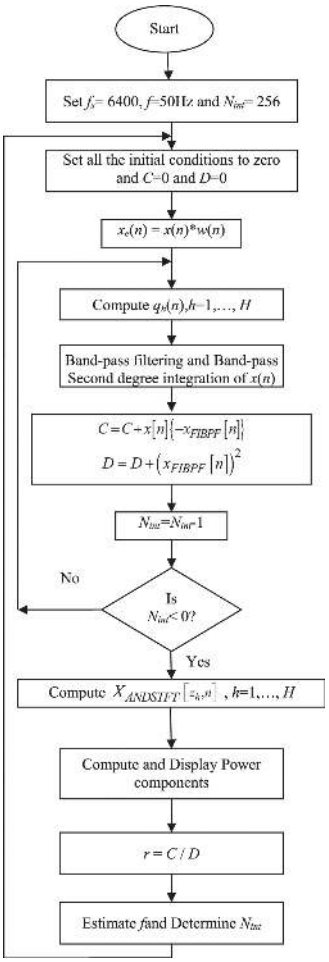

References

[1] IEEE standard definitions for the measurement of electric power quantities under sinusoidal, nonsinusoidal, balanced or unbalanced conditions. IEEE Standard, Mar 2010:1459–2010.
[2] Pejic D, Naumovic-Vukovic D, Vujicic B, Radonjic A, Sovilj P, Vujicic V. Stochastic digital DFT processor and its application to measurement of reactive power and energy. Meas. 2018;124:494–504.
[3] Zhuang S, Zhao W, Wang Q, Huang S. Four harmonic analysis and energy metering algorithms based on a new cosine window function. Journal Eng. 2017;2017:2678–84.
[4] Ferreira SC, Gonzatti RB, Silva CH, da Silva LE, Pereira RR, Lambert-Torres G. Adaptive real-time power measurement based on IEEE standard 1459–2010. Electr Power Compon Syst. 2015;43:1307–17.
[5] Jain NL, Priyanka R, Keerthy P, Maya P, Babu P. Empirical wavelet transform for harmonic detection under dynamic condition. In: Circuit, Power and Computing Technologies (ICCPCT), 2017 International Conference on. IEEE, Apr 2017:1–5.
[6] Saleh SA. The extended Newton-phaselet method for determining the reactive power from the active power in single-phase systems. IEEE Trans Ind Appl. 2016;52:1297–307.
[7] Carugati I, Orallo CM, Donato PG, Maestri S, Strack JL, Carrica D. Three-phase harmonic and sequence components measurement method based on mSDFT and variable sampling period technique. IEEE Trans Instrum Meas. 2016;65:1761–72.
[8] Goswami S, Sarkar A, Sengupta S. Power components measurement using S-ADALINE. Int J Eng Innovations Res (IJEIR). 2017;6:120–6.
[9] De Jesus MA, Teixeira M, Vicente L, Rodriguez Y. Nonuniform discrete short-time fourier transform a goertzel filter bank versus a FIR filtering approach. In: Circuits and Systems, 2006. MWSCAS'06. 49th IEEE International Midwest Symposium on. vol. 2. IEEE, 2006:188–92.
[10] Sarkar A, Sengupta S. The nonuniform discrete short time fourier transform – a new tool for electrical power components' monitoring. In: Processing Joint International Conference on Power System Technology and IEEE Power India Conference (POWERCON 2008). New Delhi, India, Oct 2008:1–8.
[11] Sarkar A, Sengupta S. Bandpass second-degree digital-integrator-based power system frequency estimation under nonsinusoidal conditions. Instrum Meas IEEE Trans Instrum Meas. 2011;60:846–53.
[12] Wen H, Li C, Yao W. Power system frequency estimation of sine-wave corrupted with noise by windowed three-point interpolated DFT. IEEE Trans Smart Grid. 2017;9:5163–72.

[13] Bagchi S, Mitra SK. The nonuniform discrete Fourier transform and its applications in signal processing. Springer Science & Business Media, 2012.
[14] Jaiswal S, Ballal MS. FDST-based PQ event detection and energy metering implementation on FPGA-in-the-loop and NI-LabVIEW. IET Sci Meas Technol. 2017;11:453–63.